Journal of Thermal Analysis, Vol. 47 (1996) 957-973

THERMODYNAMIC TRANSITION PROPERTIES OF HIGHLY ORDERED SMECTIC PHASES
Series of main-chain liquid crystalline polyethers

Y. Yoon, R.-M. Ho, F. Li, B. Moon, D. Kim, J.-Y. Park, F. W. Harris, S. Z. D. Cheng, V. Percec[1] and P. Chu[1]*

Maurice Morton Institute and Department of Polymer Science, The University of Akron, Akron, Ohio 44325-3909
[1]Department of Macromolecular Science, Case Western Reserve University, Cleveland, Ohio 44106-2699, USA

Abstract

A series of polyethers have been synthesized from 1-(4-hydroxy-4'-biphenyl)-2-(4-hydroxyphenyl)propane and α, ω-dibromoalkanes having different numbers of methylene units [TPPs]. Both odd- and even-numbered TPPs [TPP(n=odd)s and TPP(n=even)s) exhibit multiple transitions during cooling and heating and they show little supercooling dependence, indicating close-to-equilibrium nature of these transitions. Combining the structural characterization obtained *via* wide angle X-ray diffraction powder and fiber patterns at different temperatures and the morphological observations from microscopy techniques, not only the nematic liquid crystalline phase but also highly ordered smectic F, smectic crystal G and H phases have been identified. The phase diagrams for both TPP(n=odd)s and TPP(n=even)s have been constructed [1–3]. Thermodynamic properties (enthalpy and entropy changes) during these transitions are studied based on differential scanning calorimetry experiments. The contributions of the mesogenic groups and methylene units to each ordering process can be separated and they indicate the characteristics of these processes thereby providing estimations of the transition types.

Keywords: DSC, Gibbs energy, liquid crystalline polyethers

Introduction

The classification of the distinct liquid crystalline phases in small-molecule liquid crystals has been well established (Fig. 1) [4, 5]. The least ordered liquid crystalline phase is the nematic (N) phase which only possesses molecular orientational order due to the anisotropy of the molecular geometric shape. The smectic A (S_A) or smectic C (S_C) phase introduces a layer structure in addition to the molecular orientation. In the S_A phase the molecular long axis is parallel

* Author to whom all correspondence should be addressed.

0368–4466/96/ $ 5.00

John Wiley & Sons, Limited
Chichester

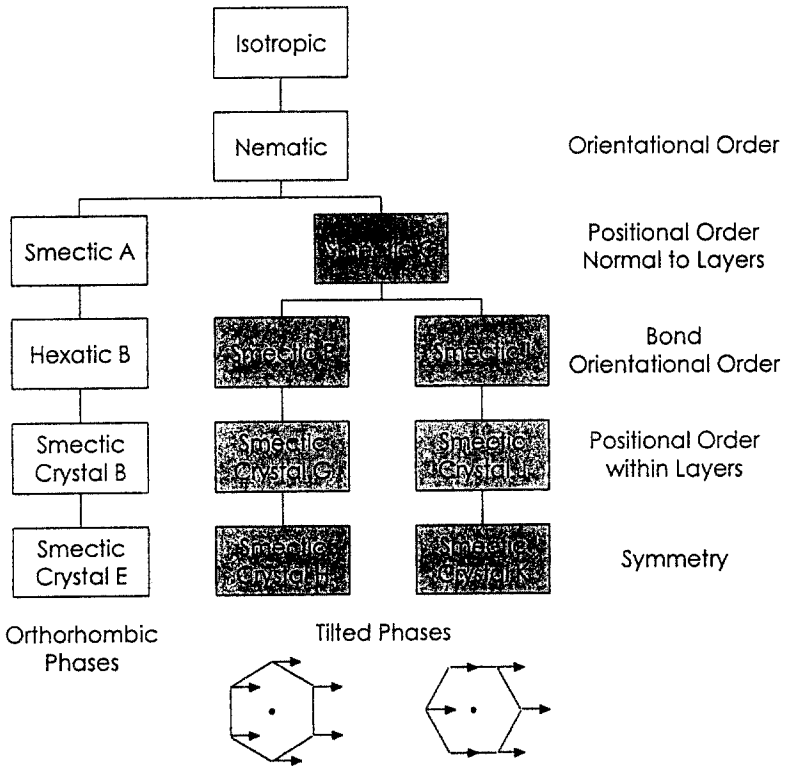

Fig. 1 Classification of the liquid crystalline phases

to the layer normal while in the S_C phase this axis is tilted away from the layer normal. Following the S_A phase the hexatic B (H_B), smectic crystal B (S_B) and smectic crystal E (S_E) phases are observed. In this series the long axis of the molecules is oriented perpendicular to the layer surface while order is increasingly developed from positional order normal to the layer in S_A, bond orientational order in H_B, positional order within the layers in S_B and, finally, asymmetric axial site symmetry in S_E [4, 5]. After the S_C phase, two subclasses of highly ordered smectic phases are recognized. The difference between these two series lies in the tilt directions: the smectic F (S_F), smectic crystals G (S_G) and H (S_H) possess the long axis tilted towards one side while the long axis directions in the smectic I (S_I), smectic crystals J (S_J) and K (S_K) are tilted towards one apex (Fig. 1). The development of order in both cases is correspondingly identical as in the first series from S_A to S_E. Furthermore, the S_F, S_G, S_I and S_J phases exhibit hexagonal packing when viewed parallel to the long axis. The packing of the tilted long axis leads to a monoclinic lattice (for S_F and S_G phases $a > b$ and for S_I and S_J phases $a < b$). In the S_H and S_K phases, an orthorhombic, herringbone type of packing exists [4, 5]. To identify these highly ordered smectic phases in small-molecule liquid crystals, wide angle X-ray diffraction

(WAXD), calorimetry, polarized light microscopy (PLM) and phase mixing experiments are usually utilized [4].

In the last two decades, efforts have been made on understanding the transition behavior of the main-chain liquid crystal polymers [6]. It has been known that a liquid crystal transition from the isotropic melt usually exhibits a thermodynamic first-order transition [7], which is defined that the first derivatives of the Gibbs energy are discontinuous, and occurs close-to-equilibrium. This behavior is reflected by the cooling-rate independence of the transition. Such behavior can be easily determined through differential scanning calorimetry (DSC). On the other hand, structural changes during the transition can be characterized *via* WAXD powder and fiber experiments. In some cases, quantitative descriptions of defects may be obtained from PLM. For semicrystalline polymers having a liquid crystal state, the 'lamellar decoration' method using transmission electron microscopy (TEM) [8, 9] has also been developed to establish relationships between molecular characteristics, such as chain rigidity, molecular weight, and Frank constants. Molecular motions in different liquid crystal phases have also been investigated *via* ^{13}C-solid state nuclear magnetic resonance. The nematic phase has been the most commonly reported phase in main-chain liquid crystalline polymers. Recently, some studies have shown that S_A, S_C or higher ordered smectic phases may also be possible in these polymers [10–14]. The difference between polymers and small-molecule liquid crystals is the covalent connectivity existing in the polymer case. Despite this difference we can show that highly ordered S_F, S_G and S_H phases are also found in a series of main-chain liquid crystalline polyethers.

Experimental section

Materials

The polyethers were synthesized from 1-(4-hydroxy-4'-biphenyl)-2-(4-hydroxyphenyl)propane (TPP) and α, ω-dibromoalkanes. The detailed synthetic procedure has been reported in an earlier publication [15]. Molecular weights of the samples were ranged between 20 000 and 50 000 based on gel permeation chromatography experiments using polystyrene as standards. The chemical structure of the TPPs is shown below:

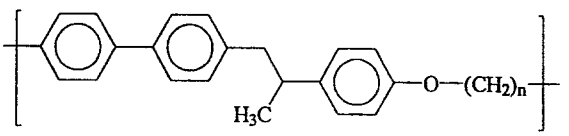

Instrument and experiments

DSC experiments were carried out in a Perkin-Elmer DSC-7. The temperature and heat flow scales at different cooling and heating rates (2.5–40°C min^{-1}) were

carefully calibrated using standard materials. Typically, the DSC sample size was 2–3 mg. When fast cooling and heating rates were applied the sample weight was reduced to less than 0.5 mg to avoid thermal gradients within the samples. The samples were heated to above their melting temperatures and hold there for two minutes and then cooled to below the glass transition temperature at different cooling rates. The consecutive heating was also performed at a rate which was equal to or faster than the prior cooling rate. When the DSC cooling curves were used to analyze the transition behavior, the onset temperature of the transition in the high temperature side was determined. When the heating curves were used, the onset temperature was found from the low temperature side. When the peaks were overlapped, those were resolved using PeakFit program published by Jandel Scientific. Asymmetric double sigmoidal function was used for the peak resolution.

Wide angle X-ray diffraction (WAXD) experiments were performed on a Rigaku 12 kW rotating anode generator (CuK_α radiation) equipped with a Siemens two-dimensional area detector with built-in hot stage to determine the temperature dependence of the unit cell dimensions. The refinement of unit cell dimension was carried out *via* a program developed in our laboratory.

Results and discussion

Figures 2a and 2b show phase diagrams for TPP(n=odd)s and TPP(n=even)s, respectively [1–3]. Due to the well-known odd-even effect of the methylene units, the transition temperatures and phase boundaries of the diagrams are significantly different. It is important that the transition temperatures in these phase diagrams must be in thermodynamic equilibrium. Based on our DSC results at different cooling and heating rates in the range between 2.5 and 40°C min^{-1}, these phase transitions in this series of polyethers show little supercooling and superheating dependence as shown in Figs 3 to 6 for TPP(n=11, 17, 8 and 16), respectively, as examples [1–3]. This is a clear indication that these transitions are close-to-equilibrium. With increasing the number of methylene units a tendency of slightly increasing supercooling or superheating may be found. Additionally, the enthalpy change for each transition is also almost cooling- or heating-rate independent [1–3], which further reveals the equilibrium status of the phase transitions. The enthalpy and entropy changes at each phase transition in the liquid crystalline states for all the TPPs are listed in Table 1. The supercooling of each transition in the cooling-rate range between 2.5 and 40°C min^{-1} is also included in this table. Since the DSC results provide precise information about the heat release or absorption during the transitions, sudden change in enthalpy, entropy and volume at the transition manifests the nature of the first-order transitions based on the thermodynamic definition [7]. It should be aware that however, DSC experiments do not give

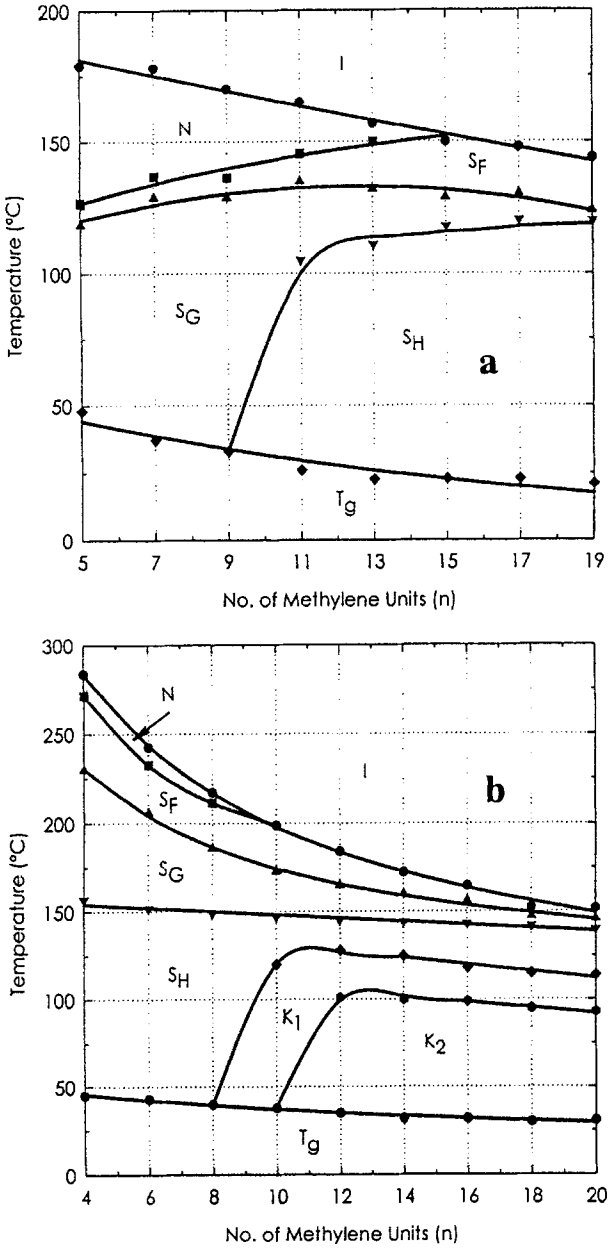

Fig. 2 Phase diagram of (a) TPP(n=odd)s and (b) TPP(n=even)s

rise to information of the structural changes during these transitions. As a result, the assignment of each phase in Figs 2a and 2b has to be identified *via* structural characterizations such as WAXD and electron diffraction (ED) ex-

Table 1 The transition enthalphy and entropy changes of TPPs at each phase transition temperature

n	$I \rightarrow N$		I or $N \rightarrow S_F$		$S_F \rightarrow S_G$		$S_G \rightarrow S_H$	
	ΔH	ΔS	ΔH	ΔS	ΔH	ΔS	ΔH	ΔS
4	6.66	11.96	7.85	14.21	3.74	7.44	3.58	8.42
5	4.74	10.48	2.68	6.70	1.99	5.08	–	–
6	7.35	14.25	8.05	15.92	4.35	9.00	5.49	13.38
7	6.21	13.76	3.45	8.40	2.78	6.92	–	–
8	8.20	16.73	8.46	17.46	4.95	10.69	7.39	17.14
9	7.34	16.56	4.24	10.34	3.77	9.36	–	–
10	–	–	17.92	37.97	5.70	12.58	9.30	22.86
11	8.48	19.36	5.23	12.50	4.71	11.54	10.15	25.89
12	–	–	18.84	41.20	6.45	14.90	11.20	26.61
13	9.94	23.11	6.40	14.28	5.58	13.78	11.96	30.84
14	–	–	19.87	44.61	7.05	16.59	13.11	30.99
15	–	–	18.14	42.15	6.21	15.44	13.69	35.01
16	–	–	20.90	47.73	7.65	18.08	15.01	35.66
17	–	–	20.20	46.96	7.71	17.53	15.50	40.37
18	–	–	22.13	51.99	8.25	19.72	16.92	40.76
19	–	–	22.43	52.17	8.56	19.55	17.21	44.66
20	–	–	23.25	54.72	8.84	21.25	18.82	45.59

ΔH is in kJ mol^{-1} and ΔS is in J $(K\ mol)^{-1}$

periments coupled with morphological observations. Combining Table 1 and Figs 2a and 2b, it is interesting that the enthalpy and entropy changes of the transitions associated with N and S_F phases are relatively large compared with those in the transitions of S_G and S_H phases. In particular, the $S_F \rightarrow S_G$ phase transitions show very small enthalpy and entropy changes.

The N phase is the most commonly observed phase in main-chain liquid crystalline polymers. This phase possesses one-dimensional orientational order along the long axis of the molecules while the lateral packing is still liquid-like. The $I \rightarrow N$ phase transition in the liquid crystalline polymers can be clearly observed *via* DSC and it shows a first-order transition with relatively small entropy and enthalpy changes during the transition [16]. From Figs 2a and 2b, the phase diagrams indicate that the $I \rightarrow N$ transition exists in odd-*TPP*($n \leq 13$)s and even-TPP($n \leq 8$)s [1–3]. Figure 7 shows the relationships between the transition enthalpy change and the number of methylene units for both TPP groups. This kind of plot was first reported by Blumstein *et al.* for another main-chain liquid crystalline polymer [17, 18]. It is clear that linear relationships of the transition properties with respect to the number of methylene units (up to

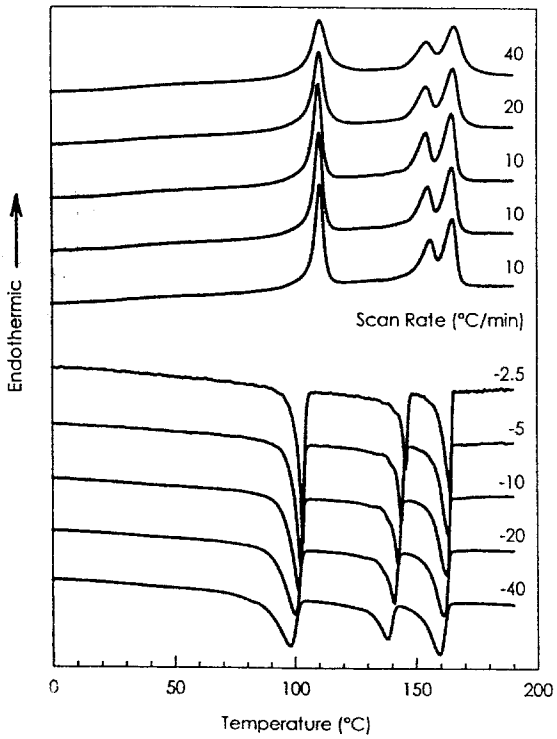

Fig. 3 Set of DSC cooling and heating curves for TPP(n=11) at different rates

n=20) are found and the enthalpy changes for the TPP(n=odd)s are relatively small compared with those in TPP(n=even)s. This is due perhaps to the odd-even effect which affects the mesogenic group packing and orientation correlation due to methylene unit conformation. Since the equilibrium transition temperatures are known from Figs 2 and 3, the entropy changes at the transitions can be calculated *via* the well-known thermodynamic relationship $\Delta S=\Delta H/T$ and shown in Fig. 8. Both Figs 7 and 8 illustrate that the nematic structure in TPP(n=even)s is more ordered than that in TPP(n=odd)s. Furthermore, the slopes in Figs 7 and 8 roughly represent the contribution to the thermodynamic transition properties per mole of methylene units while the intercepts, which are extrapolated to zero methylene unit, should be the thermodynamic properties solely attributed to the mesogenic groups. For the $I \rightarrow N$ transition, the results are listed in Table 2. The enthalpy and entropy changes of the mesogenic groups in TPP(n=even)s are much greater than those in TPP(n=odd)s [5.01 kJ mol^{-1} *vs.* 1.64 kJ mol^{-1} for the enthalpy changes and 7.65 J (K mol)$^{-1}$ *vs.* 2.80 J (K mol)$^{-1}$ for the entropy changes, respectively]. On the other hand, those changes of the methylene units in TPP(n=even)s are

slightly smaller than those in TPP(n=odd)s [0.40 kJ mol^{-1} *vs.* 0.63 kJ mol^{-1} for the enthalpy changes and 1.12 J (K mol)$^{-1}$ *vs.* 1.54 J (K mol)$^{-1}$ for the entropy changes, respectively). This reveals that the structural order in the nematic phase for TPP(n=even)s is mainly attributed to the mesogenic groups. This indicates that both the mesogenic group and methylene unit may play different roles to stable the liquid crystalline state. When the minimum energy necessary for stabling a liquid crystalline phase is determined (an ultimate thermodynamic stability of a specific phase), a balance of the contributions from both the mesogenic group and methylene unit may be achieved. A higher contribution from the mesogenic group to the energy may lead to a less interaction introduced from the methylene units. Similar observations can also be found in other main-chain liquid crystalline polymers [11].

The thermodynamic transition properties of the $I \rightarrow N$ and $N \rightarrow S_F$ transition for odd-TPP($n \leq 13$)s and even-TPP($n \leq 8$)s as well as the $I \rightarrow S_F$ transition for odd-TPP($n \geq 15$)s and even-TPP($n \geq 10$)s are shown in Figs 9 and 10. The linear relationships between these properties and the number of methylene units (similar to Figs 7 and 8) can be found. Again, the slopes and intercepts possess the same physical meanings as described above. Specifically, it is important to note

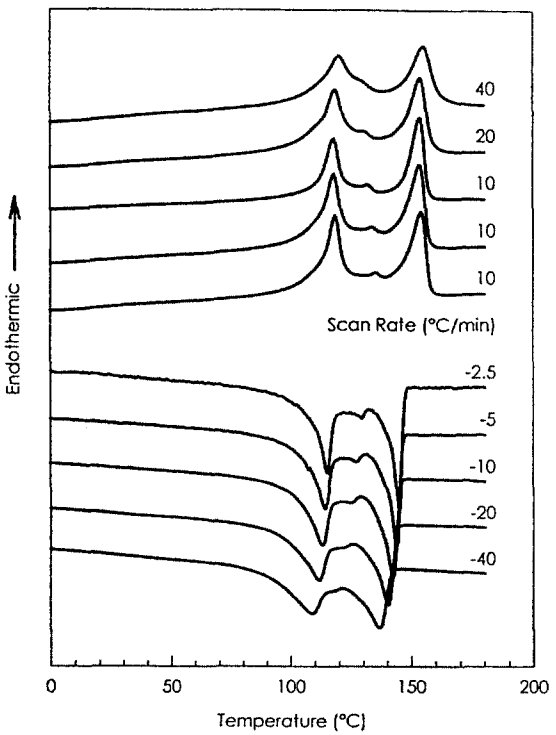

Fig. 4 Set of DSC cooling and heating curves for TPP(n=17) at different rates

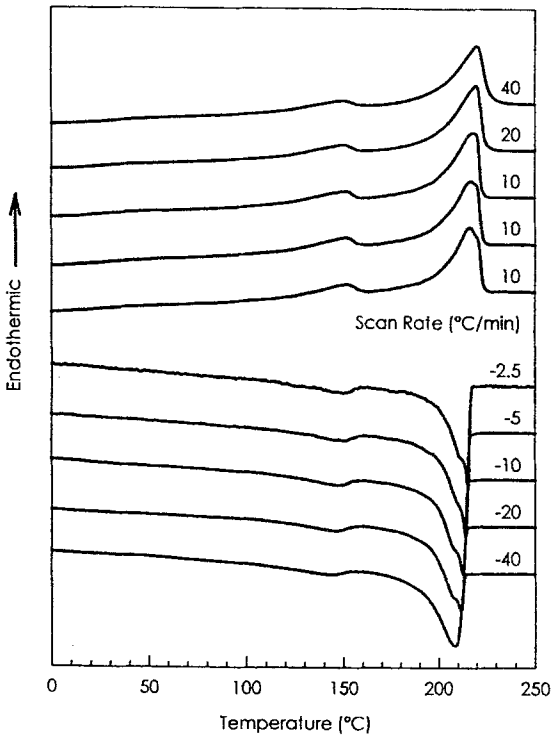

Fig. 5 Set of DSC cooling and heating curves for TPP(n=8) at different rates

that in these two figures the transition enthalpy and entropy changes for odd-TPP($n\geq15$)s and even-TPP($n\geq10$)s are only attributed to the single transition process directly from the isotropic melt (the $I \rightarrow S_F$ transition), while for odd-TPP($n\leq13$)s and even-TPP($n\leq8$)s these changes are the summation of the contributions from the two transition processes, namely, the $I \rightarrow N$ and $N \rightarrow S_F$ transitions. Surprisingly, all the data fit well into the same linear relationships. It is thus expected that an additive scheme holds in these thermodynamic properties. This indicates that Ostwald's law of successive states can be used to describe this scheme which says that a phase will occur step-by-step through successively more stable polymorphs [19]. Furthermore, the quantitative data show that the mesogenic group contributions to the enthalpy and entropy changes of this transition in TPP(n=even)s are almost five times greater than those for TPP(n=odd)s. On the other hand, the methylene unit contributions to these changes for TPP(n=odd)s are more than two times of those in TPP(n=even)s. The detailed results are listed in Table 2 for comparison.

Further cooling the TPP samples leads to the appearance of transition processes which indicates continuous ordering (Figs 2 and 3). The $S_F \rightarrow S_G$ transition can be observed in all TPP(n=odd)s and TPP(n=even)s. Figures 11

and 12 show the linear relationships between the thermodynamic transition properties with the number of methylene units and again, the data are listed in Table 2. An important observation here is that for TPP(n=odd)s the extrapolations of both the relationships to zero methylene unit (intersect) are very close to zero. This indicates that the ordering process of this $S_F \rightarrow S_G$ transition is basically attributed to the methylene units and the mesogenic groups do not contribute. However, in the cases of TPP(n=even)s, the transition enthalpy and entropy changes for the mesogenic groups are 2.45 kJ mol^{-1} and 3.85 J $(K\ mol)^{-1}$, respectively. Also, note the non-zero contribution from the methylene units (Table 2). This reveals that the formation mechanism of this S_G phase in TPP(n=odd)s is intrinsically different from that in TPP(n=even)s. Note that the small enthalpy changes in this transition fit well with the observations of this transition in small-molecule liquid crystals [4]. Furthermore, it is evident that the $S_F \rightarrow S_G$ phase transition is not a second- or even higher-order transition as speculated previously.

From WAXD experiments, it is also interesting to find that the unit cell dimensions along the a- and b-axes show small, but sudden, changes at the transition temperature of the $S_F \rightarrow S_G$. Their first derivatives with respect to the temperature, the coefficients of thermal expansion of those axes, also exhibit dis-

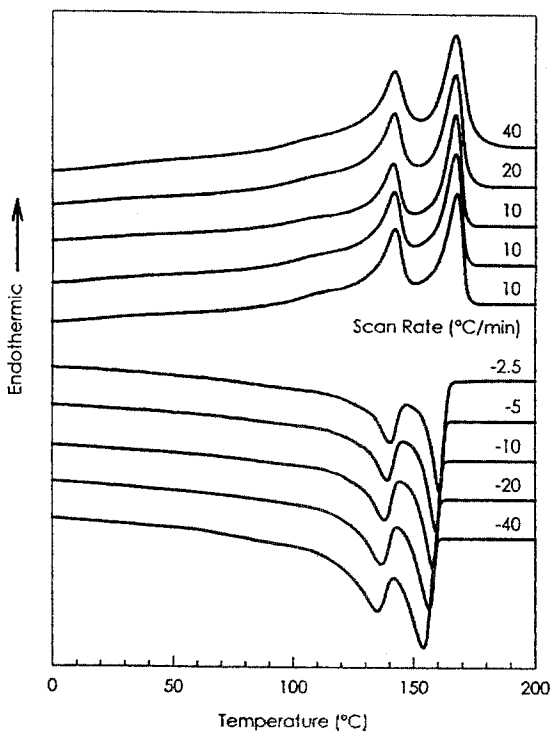

Fig. 6 Set of DSC cooling and heating curves for TPP(n=16) at different rates

continuous changes [20]. This clearly indicates that the $S_F \rightarrow S_G$ transition possesses the characteristics of a thermodynamic first-order transition [7]. Figure 13 shows the *a*- and *b*-axis changes for TPP(n=9) as an example. From Fig. 2a, it is

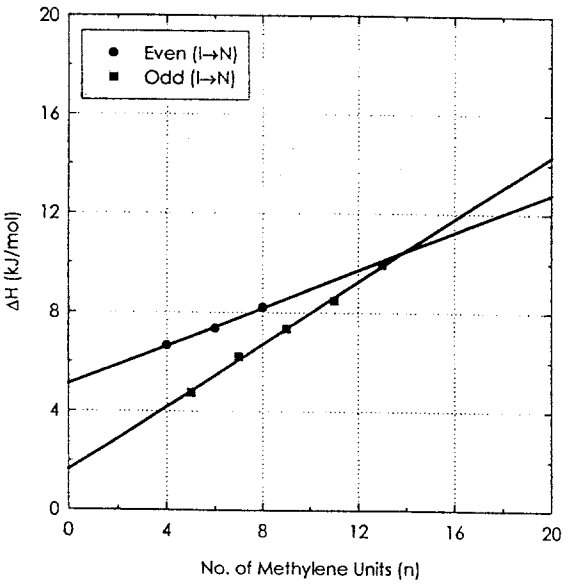

Fig. 7 Relationship of enthalpy change at I → N transition with the number of methylene units for TPP(n=odd)s and TPP(n=even)s

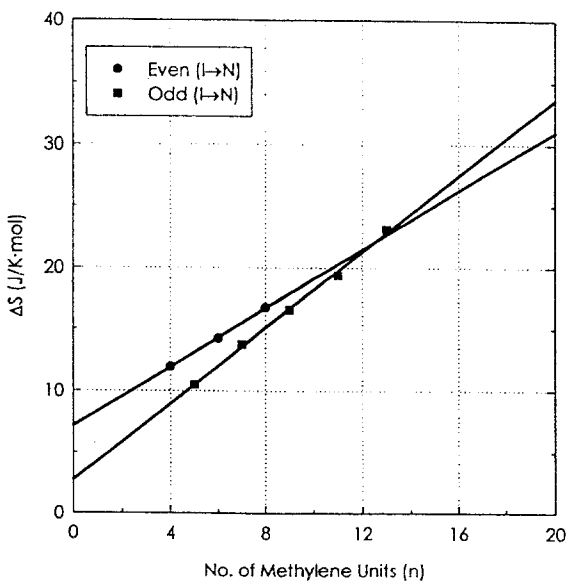

Fig. 8 Relationship of entropy change at $I \rightarrow N$ transition with the number of methylene units for TPP(n=odd)s and TPP(n=even)s

clear that the $S_F \rightarrow S_G$ transition occurs at 129°C. Below 129°C down to the glass transition temperature no transition can be observed in the DSC experi-

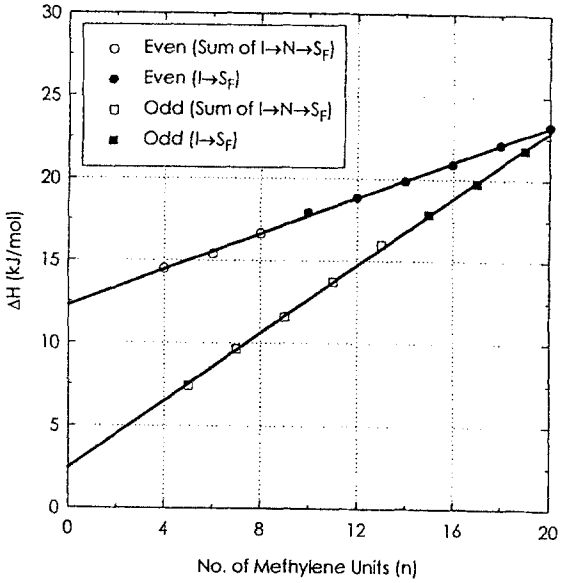

Fig. 9 Relationship of enthalpy change at $I \rightarrow S_F$ transition with the number of methylene units for TPP(n=odd)s and TPP(n=even)s

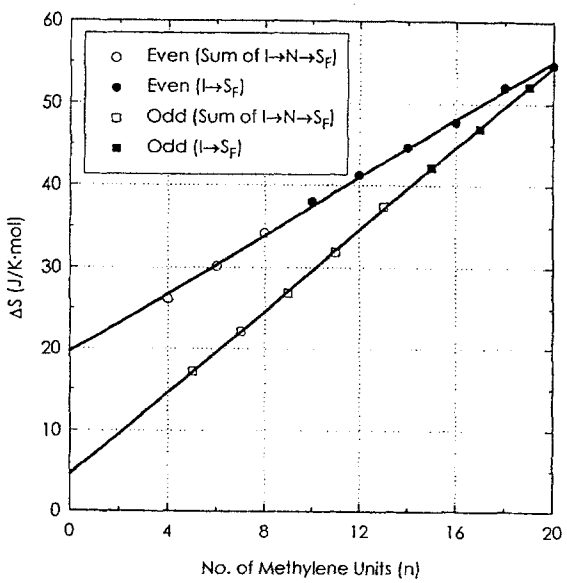

Fig. 10 Relationship of entropy change at $I \rightarrow S_F$ transition with the number of methylene units for TPP(n=odd)s and TPP(n=even)s

ments. This indicates that the S_G phase is retained down to the glassy state. In the S_G phase, the dimensional change of the a-axis ($8.9\times10^{-4}\pm0.3\times10^{-4}$ nm/°C)

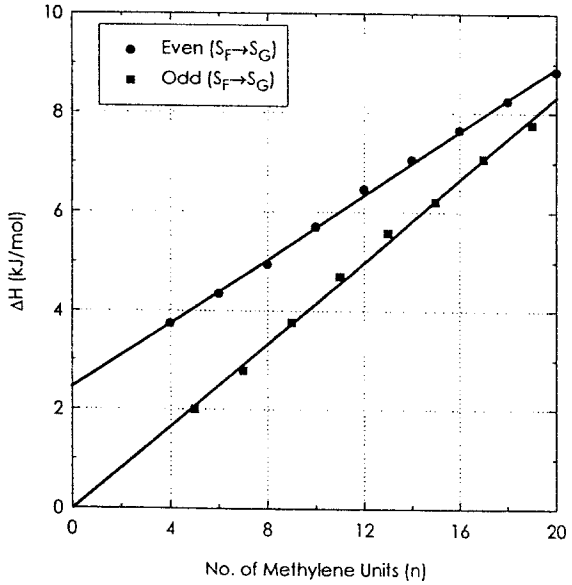

Fig. 11 Relationship of enthalpy change at $S_F \rightarrow S_G$ transition with the number of methylene units for TPP(n=odd)s and TPP(n=even)s

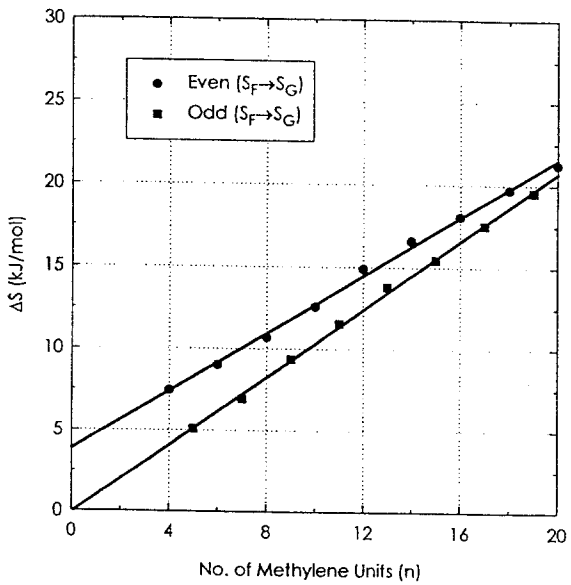

Fig. 12 Relationship of entropy change at $S_F \rightarrow S_G$ transition with the number of methylene units for TPP(n=odd)s and TPP(n=even)s

is greater than that of the b-axis ($1.10\times10^{-4} \pm 0.3 \times10^{-4}$ nm/°C) and these changes are caused by thermal expansion since linear changes of the dimensions with temperature are found (Fig. 13). This implies that constant coefficients of thermal

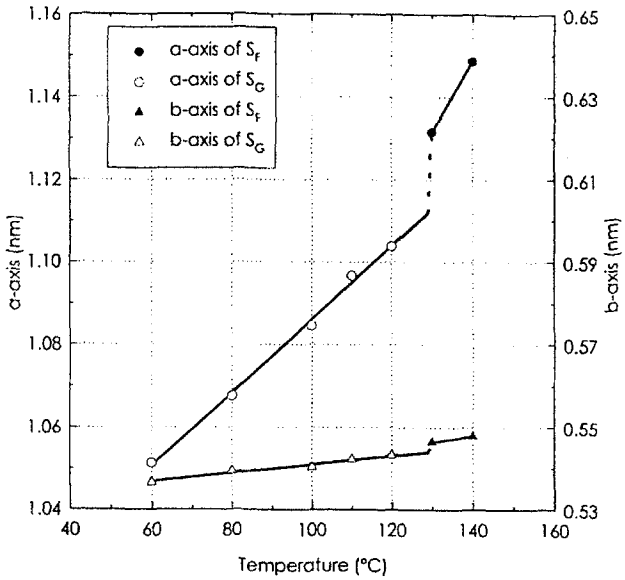

Fig. 13 Thermal expansions of a- and b-axes in the S_G and S_F phases in TPP(n=9)

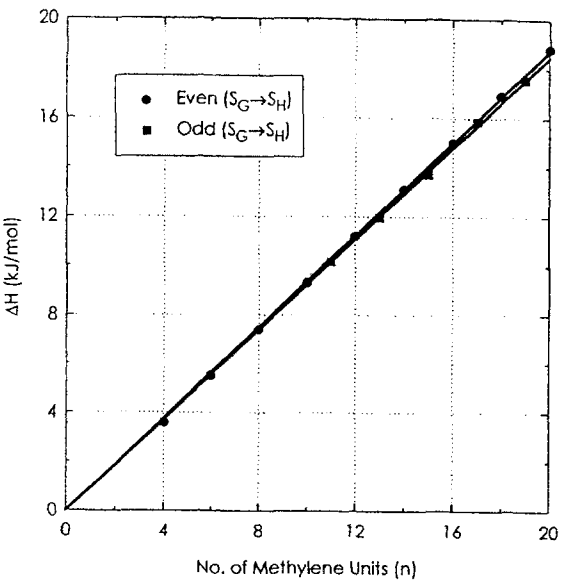

Fig. 14 Relationship of enthalpy change at $S_G \rightarrow S_H$ transition with the number of methylene units for TPP(n=odd)s and TPP(n=even)s

Table 2 The transition enthalpy and entropy changes for methylene units and mesogenic groups for the liquid crystalline transitions

		ΔH/kJ mol^{-1}		ΔS/J (K mol)$^{-1}$	
	Transition	Mesogene	Methylene	Mesogene	Methylene
	$I \rightarrow N$	1.64	0.63	2.80	1.54
	$N \rightarrow S_F$	0.50	0.43	1.78	0.96
Odd	$I \rightarrow S_F$	2.14	1.06	4.58	2.50
	$S_F \rightarrow S_G$	≈0.00	0.42	≈0.00	1.04
	$S_G \rightarrow S_H$	≈0.00	0.92	≈0.00	2.35
	$I \rightarrow N$	5.01	0.40	7.65	1.12
	$N \rightarrow S_F$	7.15	0.16	11.43	0.73
Even	$I \rightarrow S_F$	12.16	0.56	19.14	1.81
	$S_F \rightarrow S_G$	2.45	0.32	3.85	0.89
	$S_G \rightarrow S_H$	≈0.00	0.95	≈0.00	2.25

expansion (CTE) for each axis exist. Above the temperature of 129°C, TPP(n=9) enters the S_F phase and another set of linear CTE for both the a- and b-axes ($1.71\times10^{-3}\pm0.3\times10^{-4}$ nm/°C *vs.* $1.40\times10^{-4}\pm0.3\times10^{-4}$ nm/°C) can be observed (Fig. 13). Discontinuous changes at 129°C between the dimensional changes in the S_F and S_G phases indicate that the $S_G \rightarrow S_F$ transition is a thermodynamically first order transition. This reveals that, in the S_G or S_F phase,

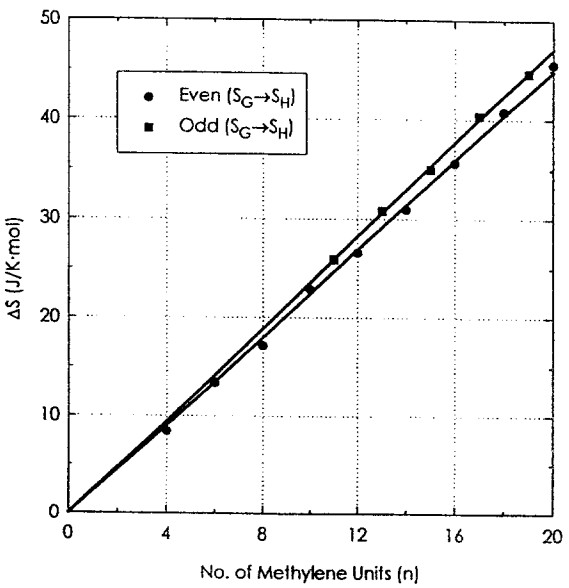

Fig. 15 Relationship of entropy change at $S_G \rightarrow S_H$ transition with the number of methylene units for TPP(n=odd)s and TPP(n=even)s

the a-axis expands almost one order of magnitude greater than the b-axis. In addition, the coefficients of thermal expansion for both the a- and b-axes in the S_F phase are about 2 and 1.3 times greater than those in the S_G phase, respectively, thus revealing that the S_G phase retains more solid nature than the S_F phase. This observation provides additional evidence for the DSC observations and phase assignment.

For TPP(n=odd)s, the S_G phase is retained down to their glass transition temperatures for $n \leq 9$. Only TPP(n(11))s show the $S_G \rightarrow S_H$ transition (Fig. 2). On the other hand, all TPP(n=even)s possess this transition. Figures 14 and 15 show the linear relationships between thermodynamic transition properties and the number of methylene units. It is important to find that the mesogenic groups in all the TPPs do not contribute to the enthalpy change during this transition. This indicates that the ordering process is solely attributed to the methylene units. Moreover, the quantitative values of the contributions for both series of TPP(n=odd)s and TPP(n=even)s are close to each other (Table 2).

Conclusion

In summary, TPPs show complicated phase transition behaviors. Based on the phase diagrams are established, the thermodynamic transition properties of various phases obtained from DSC are discussed. It is evident that the concepts of highly order smectic phases developed in small-molecule liquid crystals can also be utilized in the main-chain liquid crystalline polymers.

* * *

This work was supported by the SZDC's Presidential Young Investigator Award from the National Science Foundation (DMR-9175538). The generous donation of a DSC-7 from Perkin Elmer Inc. is also greatly appreciated.

References

1 Y. Yoon, A. Zhang, R.-M. Ho, S. Z. D. Cheng, V. Percec and P. Chu, Macromolecules, 29 (1996) 294.
2 Y. Yoon, B. Moon, D. Kim, K. W. McCreight, F. W. Harris, S. Z. D. Cheng, V. Percec and P. Chu, Macromolecules, 29 (1996) 3421.
3 Y. Yoon, Ph.D. Dissertation, Department of Polymer Science, The University of Akron, Akron, Ohio, 44325-3909, 1995.
4 G. W. Gray, J. W. G. Goodby, Smectic Liquid Crystals, Leonard Hill, London 1984.
5 P. S. Pershan, Structure of Liquid Crystal Phases, World Scientific, NJ 1988.
6 For a recent review, see for example, V. Percec, D. Tomazos, In Comprehensive Polymer Science, First Supplement; G. Allen, S. L. Aggarwal and S. Russo, Eds. Pergamon, Oxford 1992, pp. 300-356. In this review, over four hundred references were collected.
7 P. Ehrenfest, Proc. Acad. Sci. Amsterdam, 36 (1933) 153.
8 E. L. Thomas and B. A. Wood, Faraday Discuss. Soc., 79 (1985) 229.
9 B. A. Wood and E. L. Thomas, Nature, 324 (1986) 655.
10 W. R. Krigbaum, J. Asrar, H. Toriumi, A. Ciferri and J. Preston, J. Polym. Sci. Polym. Lett., (1982) 20, 109.

11 R. Pardey, F. W. Harris, S. Z. D. Cheng, J. Aducci, J. V. Facinelli and R. W. Lenz, Macromolecules, 25 (1992) 5060; 26 (1993) 3687.
12 J. Watanabe, M. Hayashi, A. Morita and T. Niiori, Mol. Cryst. Liq. Cryst., 254 (1994) 221.
13 A. Coassolo, M. Foá, D. Dainelli, R. Scordamaglia, L. Barino, L. L. Chapoy, F. Rustichelli, B. Yang and G. Torquati, Macromolecules, 24 (1991) 1701.
14 M. Carotenuto and P. Iannelli, Macromolecules, 25 (1992) 4373.
15 V. Percec, P. Chu, G. Ungar, S. Z. D. Cheng and C.-Y. Yoon, J. Mater Chem., 4 (1994) 719.
16 B. Wunderlich and J. Grebowicz, Adv. Polym. Sci., 60/61 (1984) 1.
17 A. Blumstein and O. Thomas, Macromolecules, 15 (1982) 1264.
18 R. B. Blumstein and A. Blumstein, Mol. Cryst. Liq. Cryst., 165 (1988) 361.
19 W. Ostwald, Z. Physik. Chem., 22 (1897) 286.
20 S. Z. D. Cheng, Y. Yoon, A.-Q. Zhang, E. P. Savitski, J.-Y Park, V. Percec and P. Chu, Macromol. Rapid Commun., 16 (1995) 533.